Science Bulletin 66 (2021) 1906–1916

Contents lists available at ScienceDirect

Science Bulletin

journal homepage: www.elsevier.com/locate/scib

Article

Complete biosynthesis of the potential medicine icaritin by engineered *Saccharomyces cerevisiae* and *Escherichia coli*

Pingping Wang [a,1], Chaojing Li [a,b,1], Xiaodong Li [a,b,1], Wenjun Huang [c,1], Yan Wang [a], Jiali Wang [a,d], Yanjun Zhang [c], Xiaoman Yang [e], Xing Yan [a,b,*], Ying Wang [b,e,*], Zhihua Zhou [a,b,*]

[a] *CAS-Key Laboratory of Synthetic Biology, CAS Center for Excellence in Molecular Plant Sciences, Institute of Plant Physiology and Ecology, Chinese Academy of Sciences, Shanghai 200032, China*
[b] *University of Chinese Academy of Sciences, Beijing 100049, China*
[c] *Key Laboratory of Plant Germplasm Enhancement and Specialty Agriculture, Wuhan Botanical Garden, Chinese Academy of Sciences, Wuhan 430074, China*
[d] *School of Life Sciences, Henan University, Kaifeng 475001, China*
[e] *Key Laboratory of South China Agricultural Plant Molecular Analysis and Genetic Improvement, Center of Economic Botany/Core Botanical Gardens, South China Botanical Garden, Chinese Academy of Sciences, Guangzhou 510650, China*

ARTICLE INFO

Article history:
Received 30 October 2020
Received in revised form 12 December 2020
Accepted 8 February 2021
Available online 7 March 2021

ABSTRACT

Icaritin is a prenylflavonoid present in the Chinese herbal medicinal plant *Epimedium* spp. and is under investigation in a phase III clinical trial for advanced hepatocellular carcinoma. Here, we report the biosynthesis of icaritin from glucose by engineered microbial strains. We initially designed an artificial icaritin biosynthetic pathway by identifying a novel prenyltransferase from the *Berberidaceae*-family species *Epimedium sagittatum* (EsPT2) that catalyzes the C8 prenylation of kaempferol to yield 8-prenlykaempferol and a novel methyltransferase GmOMT2 from soybean to transfer a methyl to C4'-OH of 8-prenlykaempferol to produce icaritin. We next introduced 11 heterologous genes and modified 12 native yeast genes to construct a yeast strain capable of producing 8-prenylkaempferol with high efficiency. GmOMT2 was sensitive to low pH and lost its activity when expressed in the yeast cytoplasm. By relocating GmOMT2 into mitochondria (higher pH than cytoplasm) of the 8-prenylkaempferol–producing yeast strain or co-culturing the 8-prenylkaempferol–producing yeast with an *Escherichia coli* strain expressing GmOMT2, we obtained icaritin yields of 7.2 and 19.7 mg/L, respectively. Beyond the characterizing two previously unknown plant enzymes and conducting the first biosynthesis of icaritin from glucose, we describe two strategies of overcoming the widespread issue of incompatible pH conditions encountered in basic and applied bioproduction research. Our findings will facilitate industrial-scale production of icaritin and other prenylflavonoids.

1. Introduction

The group of *Berberidaceae* family plants *Epimedium* spp. are the basis of the traditional Chinese herbal medicine known internationally as *Herba Epimedii*, which has been traditionally used as a kidney tonic, aphrodisiac, anti-rheumatic, and treatment for osteoporosis [1–4]. The major bioactive compounds of *Herba Epimedii* are known to be prenylflavonoids, mainly icaritin and its derivatives [5]. Pharmacological studies have demonstrated that icaritin confers neuroprotective, cardiovascular protective, and anti-osteoporosis effects, so it was understood as a promising candidate for therapeutic applications [6,7]. Moreover, multiple studies have demonstrated that icaritin can inhibit hepatocellular carcinoma (HCC) initiation and malignant growth, while others have shown that icaritin can induce acute myeloid leukemia cell apoptosis [8,9]. Recently several phase III clinical trials of icaritin for treatment of advanced HCC have been ongoing (trial registration No. NCT03236649, CTR20170667, and CTR20170668) based on the conclusion of phase I (trial registration No. NCT02496949) and phase II (trial registration No. NCT01972672) clinical trials [10,11]. During the phase I clinical trial of icaritin, the treatment of 15 patients with advanced HCC, 46.7% (7 patients) achieved a clinical benefit (1 partial response and 6 stable disease), and there were no observed drug-related adverse events ($\geq$ Grade 3) in any of the enrolled patients [10]. During a single-arm, multicenter phase II clinical trial of icaritin to treat advanced HCC patients, icaritin could induce immunomodulatory of the 68 enrolled patients and thus improve the median overall survival with no

* Corresponding authors.
E-mail addresses: yanxing@sibs.ac.cn (X. Yan), yingwang@scib.ac.cn (Y. Wang), zhouzhihua@sippe.ac.cn (Z. Zhou).
[1] These authors contributed equally to this work.

https://doi.org/10.1016/j.scib.2021.03.002
2095-9273/

drug-related adverse events [11]. The phase I and phase II clinical trials showed that icaritin could have promising survival benefits for advanced HCC patients [10,11].

Currently, *Epimedium* plants are the only source of commercially available icaritin, and wild epimedium resources have been nearly depleted to exhaustion due to over-exploitation in recent years [12]. Exacerbating this issue, *Epimedium* plants are slow-growing, difficult to propagate, and have strict growth requirements (wild epimedium is mainly found in cliffs in moist forests, near streams and wet lands at specific altitudes), making the large-scale cultivation of *Epimedium* plants highly challenging [1]. Additionally, content of the natural product icaritin is <2% of dry plant matter, making the isolation and purification of bioactive components from a large amounts of plant material difficult [5]. In recent years, the total synthesis of icaritin has been realized by chemical approaches; however, this method required a long reaction route (9 steps), high temperature (190 °C), strong acid, and the use of heavy metal (Palladium on active carbon, Pd/C), which has hindered its scale-up and commercial application [13].

Metabolic engineering and synthetic biology methods offer an alternative, potentially sustainable way to produce natural products, as for examples demonstrated for artemisinic acid, ginsenosides, and many flavonoids that have been obtained via microbial fermentation [14–17]. The complete biosynthetic pathway of naringenin (NAR) was assembled and optimized in *Escherichia coli* (*E. coli*), and a strain was reported that produced 100.6 mg/L NAR directly from glucose [18]. *S. cerevisiae* has a complete intracellular membrane system and thus has advantages over *E. coli* for the expression of membrane proteins. By assembling flavonoid biosynthetic enzymes from different sources in *Saccharomyces cerevisiae* (*S. cerevisiae*), Trantas et al. [19] realized the *de novo* production of many flavonoids including NAR, kaempferol (KAE), genistein, and quercetin. The highest production of flavonoids in *S. cerevisiae* to date, which was accomplished by combining multiple pathway optimization measures, reached 220 mg/L for NAR and 86 mg/L for KAE [20]. More recently, by introducing the prenyltransferase SfFPT from *Sophora flavescens* into a NAR-producing yeast strain, a prenylated flavonoid, 8-prenylnaringenin, was produced in yeast for the first time; however, the titer was quite low (0.12 mg/L) [21]. To achieve high yields of plant natural products by microbial fermentation, especially for the natural products produced by a long synthetic pathway, the building of synthetic microbial consortium has recently been applied [22]. By dividing the long synthetic pathway into separate microbial strains, the advantages of an engineered microbial consortium could be observed, i.e., providing better environments for specific enzymes, minimizing feedback inhibition, relieving the stress from metabolic flux. A series of *E. coli–S. cerevisiae* synthetic microbial consortia were built to produce oxygenated taxanes, ferruginol and nootkatone efficiently [23]. Besides, a microbial consortia composed of *Gluconobacter oxydans*, *Bacillus* spp., and *Ketogulonicigenium vulgare* has been used for commercial vitamin C production [24].

The complete biosynthetic pathway of KAE, the precursor of icaritin, has been elucidated, and all of the genes encoding enzymes of this pathway have been identified in *Epimedium sagittatum* (*E. sagittatum*), including cinnamate-4-hydroxylase (*EsC4H*), 4-coumarate-CoA ligase (*Es4CL1-2*), chalcone synthase (*EsCHS3*), flavonol synthase (*EsFLS*) and flavanone-3-hydroxylase (*EsF3H*) [25]. There are also reports about downstream pathway enzymes that can catalyze the C3-OH-rhamnosylation and C7-OH-glucosylation of icaritin [26,27]. However, the pathway from KAE to icaritin remains elusive: the enzymes responsible for C8-prenylation and C4'-OH-methylation of the flavonoid skeletons which lead to icaritin remain to be characterized.

In this study, we developed a microbe-based approach for the synthesis of icaritin from simple sugars. We first characterized a prenyltransferase, EsPT2, from *E. sagittatum*, which catalyzes the C8 prenylation of KAE to yield 8-prenylkaempferol (8P-KAE). Next, we generated an artificial icaritin biosynthetic pathway by searching for an OMT that catalyzes the C4'-OH-methylation of 8P-KAE from the model plant *Glycine max*. By introducing 11 heterologous genes from five sources (*Arabidopsis thaliana*, (*A. thaliana*), *E. coli, Flavobacterium johnsoniae* (*F. johnsoniae*), *E. sagittatum*, and *G. max*) combined with multiple metabolic engineering measures involving the modification of 12 native genes, we obtained a series of yeast strains with increased KAE production (151.5 mg/L) and 8P-KAE production (25.9 mg/L). GmOMT2 did not produce icaritin when present in the cytoplasm of 8P-KAE–producing yeast strains, so we circumvented this issue by two independent strategies, (i) relocating GmOMT2 into the mitochondria of 8P-KAE–producing yeast strains and (ii) developing a co-culture system of the 8P-KAE–producing yeast and a GmOMT2-expressing *E. coli* strain. The use of these strategies resulted in icaritin yields of 7.2 and 19.7 mg/L, respectively. We produced icaritin from glucose using microbial strains, paving the way for industrial fermentation of icaritin and its bioactive derivatives via future optimization efforts.

2. Materials and methods

2.1. Materials, plasmids, and strains

Authentic flavonoid samples were purchased from Nantong Feiyu Biological Technology Co., Ltd. (Nantong, China). Detailed catalog numbers of flavonoid samples are provided in online information. Plant material *E. sagittatum* was obtained from South China Botanical Garden, Chinese Academy of Sciences (CAS). Other plant materials are from the Institute of Plant Physiology and Ecology, CAS. *E. coli* strain TOP10 was used for gene cloning and BL21 (DE3) was used for heterologous expression and whole-cell catalysis. *S. cerevisiae* strain CEN.PK2-1C (*MATa*; *ura3-52*; *trp1-289*; *leu2-3_112*; *his*3 *Δ1*) from EUROSCARF (www.euroscarf.de; Oberursel, Germany) was used as the parent strain for all yeast cell factories. Gene *SfFPT*, *SfN8DT-1*, and codon-optimized genes were synthesized by Genscript Corporation (Nanjing, China). All the strains and plasmids constructed in this study are listed in Table S1 (online) and the primers and genes are listed in Tables S2 and S6 (online), respectively.

2.2. Cloning, synthesis, and heterologous expression of prenyltransferases

The coding sequences of EsPT1-3 (deposited in http://npbiosys.scbit.org/ under accession No. OENC1–OENC3) were amplified from *E. sagittatum* using primer pairs EsPT1-F/R, EsPT2-F/R and EsPT3-F/R and inserted into the *Bam*HI and *Xho*I sites of pESC-HIS vector (Agilent Technologies, Santa Clara, USA), respectively. The coding sequence of SfFPT (Genbank accession No. KC513505) and SfN8DT-1 (Genbank accession No. AB325579.1) were synthesized and amplified with primer pairs SfFPT-F/R and N8DT-F/R and inserted into the *Bam*HI and *Xho*I sites of pESC-HIS vector. The resulting five plasmids were then transformed into *S. cerevisiae* strain CEN. PK2-1C, respectively. For heterologous expression of the prenyltransferase (PT) genes, the yeast strains were first grown in SC-His medium (6.7 g/L Difco yeast nitrogen base without amino acids, 20 g/L glucose, 2 g/L Drop-out mix synthetic minus histidine), then the cells were collected and incubated into SC-His induction medium (20 g/L glucose replaced with 20 g/L galactose) and grown for 48 h for protein induction.

2.3. Enzymatic assays of prenyltransferases

Microsomal protein of the PT expression yeast strains were prepared as described previously [28]. Enzymatic assays for PTs were carried out in a 100 μL volume containing 100 mmol/L Tris-HCl buffer (pH 9.0), 10 mmol/L $MgCl_2$, 200 mmol/L dimethylallyl pyrophosphate (DMAPP), 200 mmol/L naringenin, kaempferol, or kaempferide as substrate and 0.2 mg of yeast microsomal protein for 2 h in a 35 °C water bath. Reaction products were extracted by adding 100 μL ethyl acetate, the organic phase was then evaporated and dissolved in methanol for high performance liquid chromatography (HPLC) analysis. The reaction condition for determining the optimum pH of EsPT2 was the same as described above, except the reaction pH was controlled by different buffer, i. e., phosphate buffer (pH 6.0–7.5), Tris-HCl buffer (pH 7.5–9.0) and glycine buffer (pH 9.0–10.5), the reaction condition for determine the optimum temperature of EsPT2 was carried out at pH 8.5 and temperature ranged from 15 °C to 45 °C. Details for the kinetics analysis of EsPT2 are provided in Supplementary materials (online).

2.4. Heterologous expression and functional assay of methyltransferases

The coding sequences of *EsOMT1–EsOMT14* (deposited in http://npbiosys.scbit.org/ under accession No. OENC4–OENC17) and *GmOMT1–GmOMT19* (deposited in http://npbiosys.scbit.org/ under accession No. OENC18–OENC36) cloned from *E. sagittatum* and *G. max*, respectively, as well as the synthesized coding sequences of *SOMT2* and *MOMT2* were amplified by polymerase chain reaction (PCR) and inserted into the *Nco*I and *Xho*I sites of the pET28a expression vector, respectively. Heterologous expression of methyltransferase (MT) genes in *E. coli* BL21 (DE3) was induced by 0.2 mmol/L isopropyl-β-D-thiogalactopyranoside (IPTG). The cells were harvested by centrifugation and suspended in 100 mmol/L phosphate buffer (pH 8.0) supplemented with 1 mmol/L phenylmethanesulfonyl fluoride dithiothreitol (PMSF), and 1 mmol/L dithiothreitol (DTT) and disrupted using a french press (25 kpsi). Cell debris was removed by centrifugation and the supernatant was used for enzymatic assays.

Enzymatic assays for MTs were carried out in a 100 μL volume containing 100 mmol/L phosphate buffer (pH 8.0), 200 μmol/L *S*-adenosyl methionine (SAM), 200 μmol/L 8P-KAE, and 0.5 mg of crude *E. coli* MT enzymes for 2 h in a 35 °C water bath. The reaction products were extracted by adding 100 μL of ethyl acetate, and the organic phase was evaporated and dissolved in methanol for HPLC. The reaction conditions for determining the optimum pH of GmOMT2 were as described above, except that pH was controlled by adding phosphate buffer (pH 6.0–7.5), Tris-HCl buffer (pH 7.5–9.0), and glycine buffer (pH 9.0–10.5). Determination of the optimum temperature of GmOMT2 was carried out at pH 8.5 and 20 to 40 °C. The GmOMT2 kinetics analysis is described in the online information.

2.5. Construction of yeast strains

The standard procedure for each yeast strain construction was carried out as described previously [16]. Generally, this procedure contains two rounds of PCR and one transformation. The first round basic PCR was performed to amplified all the necessary bioparts (promoter, gene, terminator, selection marker and homologous arm), the adjacent primers used for first round PCR all sharing ~70 bp homologous sequences for recombination or fusion PCR. The second round fusion PCR was performed using the adjacent 2 to 4 first round basic PCR products as template to give each fusion fragments. Thirdly, the purified fusion fragments were co-transformed into yeast strain via standard LiAc/ssDNA method and integrated into chromosome via yeast homologous recombination. The primers used for all yeast strains construction are listed in Table S2 (online), and the detailed protocol for the construction of different yeast strains was described in Supplementary materials (online).

2.6. Construction of E. coli strains

Plasmid pET28a-GST-GmOMT2 was constructed by inserting glutathione S-transferase (GST) tag into the *Nco*I site of pET28a-GmOMT2, generally the GST tag was amplified from pGEX-4 T-1 with primer pairs GSTMT-F/R and ligated into the *Nco*I site of pET28a-GmOMT2 via ClonExpress II One Step Cloning Kit (Vazyme Biotech, Nanjing, China). Plasmid pET28a-GST-synGmOMT2 was constructed by replacing *GmOMT2* gene of pET28a-GST-GmOMT2 with codon-optimized *synGmOMT2*. Primer pairs for the amplification of the given genes were listed in Table S2 (online). *E. coli* strain WPE3, WPE4, and WPE5 was constructed by transformation plasmid pET28a-GmOMT2, pET28a-GST-GmOMT2, and pET28a-GST-synGmOMT2 into *E. coli* BL21 (DE3), respectively.

2.7. Strain cultivation and metabolite extraction

2.7.1. Yeast cultivation

Individual clones of each yeast strain were inoculated into 5 mL of yeast peptone dextrose (YPD) medium and cultivated overnight at 30 °C and 250 r/min. Next, the seeds were inoculated into 10 mL of YPD medium in 50 mL shake flasks at an initial A_{600nm} of 0.05 and cultured at 30 °C, 250 r/min for 96 h (NAR- and KAE-producing strains), 108 h (8P-KAE-producing strains), or 120 h (icaritin-producing strains). For cultivation of the icaritin-producing yeast strain WP137, 1 mL of 10× YPD medium (100 g/L bacto yeast extract, 200 g/L bacto peptone, and 200 g/L dextrose) was added to 10 mL of fermentation broth in 50 mL shake flasks at 48, 72, and 96 h. For flavonoid products extraction, 600 μL of fermentation broth were disrupted using a FastPrep and extracted with 600 μL of ethyl acetate; the organic phase was then evaporated and dissolved in methanol for HPLC analysis.

2.7.2. Yeast–E. coli co-cultivation

Individual yeast clones were inoculated into 5 mL of YPD medium and cultivated overnight at 30 °C and 250 r/min. The seeds were inoculated into 10 mL of YPD medium in 50 mL shake flasks at an initial A_{600nm} of 0.05 and cultured at 30 °C and 250 r/min for 72 h (A_{600nm} ~34.0). Individual *E. coli* clones were cultured in 0.5 mL of LB medium containing 100 mg/L kanamycin overnight at 37 °C and transferred to 50 mL of LB medium containing 100 mg/L kanamycin and cultivated at 37 °C until an A_{600nm} of 0.6–0.8. Next, 0.2 mmol/L IPTG was added and *E. coli* was incubated at 16 °C for 18 h. *E. coli* cells were collected, suspended in 1 mL of fresh LB medium (A_{600nm} ~18.5), added to the yeast cultures at 72 h, and co-cultivated at 30 °C for 24 h. The A_{600nm} ratio of yeast and *E. coli* used for co-culturing was about 18:1, roughly equivalent to a cell-count ratio of 1.8:1.

2.8. Chemical analysis

HPLC was performed on a Shimadzu LC20A system (Shimadzu, Kyoto, Japan) equipped with a LC20ADXR pump, an auto-sampler, and a diode array detector. Chromatographic separation of flavonoid products was carried out at 35 °C on a Shim-pack XR-ODS column (75 mm × 2.0 mm, 2.2 μm, Shimadzu). The gradient elution system consisted of 0.01% acetate acid (A) and acetonitrile (B). Separation was achieved using the following gradient: 0–2 min (15% B), 2–16 min (15%–70% B), 16–18 min (95% B), and 18–

20 min (15% B). The flow rate was maintained at 0.45 mL/min. Naringenin, dihydrokaempferol, and 8-prenylnaringenin were detected at 290 nm [29], and kaempferol, kaempferide, 8P-KAE, and icaritin were detected at 360 nm [30]. The flavonoid compounds were quantified by integrated HPLC peak area based on calibration curves of authentic reference standards of various concentrations. The conversion rate was calculated as the molar ratio of the product to total substrate. Flavonoid yields were calculated as the weight (mg) of each flavonoid per unit fermentation volume (L). To analyze chemical structures, HPLC-electrospray ionization mass spectrometry (HPLC/ESIMS) and nuclear magnetic resonance spectroscopy (NMR) analyses were performed as described in Supplementary materials (online).

3. Results and discussion

3.1. Functional characterization of a C8 prenyltransferase for flavonoids from E. sagittatum

The enzyme responsible for the C8 prenylation step of icaritin biosynthesis is unknown. Less than 20 plant PTs that use flavonoids as substrates have been reported to date, all of which are from plants of the *Fabaceae* or *Moraceae* family (Table S3 online). Among these reported flavonoid PTs, only four—SfN8DT-1, SfN8DT-2, SfN8DT-3, and SfFPT, all from *Sophora flavescens*—catalyze the C8 prenylation of NAR. However, no studies have reported that these four PTs showed activities for the C8 atom of KAE [28,31–33]. The other flavonoid PTs discovered to date catalyze C6 or C3' prenylation of flavanone or isoflavone substrates.

Based on the sequences of previously characterized plant flavonoid PTs, and specifically using their two conserved NQXXDXXXD and KD(I/L)XDX(E/D)GD motifs as queries, which were proposed by Sasaki et al. to be responsible for prenyl diphosphate recognition among plant PTs [31], we performed a BLAST search against an *E. sagittatum* transcriptome dataset (GenBank accession No. SRA008151) [25]. This identified three candidate PTs—EsPT1, EsPT2, and EsPT3—each of which had > 30% amino acid sequence similarity with other flavonoid PTs from other plant species. Analysis using the online TMHMM Server v 2.0 [34] revealed that all three of these PT candidates have seven or eight transmembrane domains, typical of plant PTs (Fig. S1 online). A phylogenetic analysis of the three candidate PTs from *E. sagittatum* and reported *Fabaceae* and *Moraceae* PTs showed that EsPT2 and EsPT3 grouped into a distinct cluster (Fig. S2 online).

The coding sequences of these three PT candidate genes were cloned into the yeast expression plasmid pESC-HIS and expressed in *S. cerevisiae*. *In vitro* enzymatic activity assays were performed wherein the microsomal fractions of the yeast strains expressing the PTs were tested with several flavonoids—NAR, KAE, and kaempferide (KDE)—as substrates, using DMAPP as a prenyl donor. Additionally, two previously reported PTs (SfN8DT-1 and SfFPT) that catalyze C8 prenylation of NAR were expressed and tested. HPLC monitoring of assay products indicated that among the five tested PTs, only the candidate EsPT2 catalyzed the C8 prenylation of KAE to produce 8P-KAE (Fig. 1a). This product was confirmed by HPLC/ESIMS (Fig. S3a online) and NMR (Fig. S4 online). Also, EsPT2 showed activity towards the other two tested substrates KDE and NAR, respectively yielding icaritin and 8-prenylnaringenin (8P-NAR) (Fig. 1b and Fig. S3b, c online). However, its conversion ratio to KDE and NAR was 8.0% and 2.4%, respectively, significantly lower than that for KAE (65.0%). By contrast, the two previously reported naringenin PTs (SfN8DT-1 and SfFPT) from *S. flavescens* and the other two PT candidates (EsPT1 or EsPT3) did not catalyze the conversion of KAE or KDE to 8P-KAE or icaritin (Fig. 1a, b). However, EsPT1 might convert KAE into other undetectable compounds under the conditions used, resulting in the significant decrease in the KAE level in the EsPT1/KAE reaction (Fig. 1b). Also, neither EsPT1 nor EsPT3 catalyzed prenylation of NAR, indicating that substrates for these enzymes were not included in the assays. SfN8DT-1 and SfFPT catalyzed the conversion of NAR to 8P-NAR, albeit at low efficiency (3.3% and 0.27%, respectively), as reported previously [31].

The optimum pH and temperature, as well as the *in vitro* enzyme kinetics, of EsPT2 were examined using KAE as the substrate. Its optimum pH was 8.0–8.5 and optimum temperature was 24–27 °C (Fig. S5 online). The V_{max}, K_m, k_{cat}, and k_{cat}/K_m values of EsPT2 were 3449.7 nmol min^{-1} mg^{-1}, 14.07 μmol/L, 2.34 s^{-1}, and 0.17 $(\mu mol/L)^{-1}$ s^{-1}, respectively (Table S4 online). Beyond the functional characterization of EsPT2 as a flavonoid PT from the *Berberidaceae* family, these results highlight EsPT2 as the first plant PT with KAE as a preferred substrate.

3.2. Identification of a methyltransferase from G. Max for the icaritin biosynthetic pathway

The finding that EsPT2 had weak activity for KDE but strong activity for KAE suggested a biosynthetic pathway, wherein an initial C8 prenylation of KAE was followed by C4'-OH methylation of 8P-KAE to generate icaritin (Fig. 1). Two flavonoid MTs, SOMT2 from *G. max* and MOMT2 from *Solanum habrochaites*, reportedly catalyze C4'-OH of several flavonoids, including NAR and KAE [35,36]. Using these two MTs as queries, we identified 14 candidate MTs from the *E. sagittatum* transcriptome dataset [25], only 10 of which were successfully cloned (EsOMT1–EsOMT10) and none catalyzed the C4'-OH of 8P-KAE or KAE (Table S5 online).

To obtain a MT biopart catalyzing the C'–OH methylation of 8P-KAE, we screened 19 newly cloned MTs (GmOMT1–GmOMT19) from *G. max*, which are deposited in the Registry and Database of Bioparts for Synthetic Biology (http://npbiosys.scbit.org/, accession nos. OENC18–OENC36) as well as two reported MTs (SOMT2 and MOMT2). Although SOMT2 and MOMT2 were previously reported to catalyze the C4'-OH methylation of NAR and KAE [36], they showed no activity with 8P-KAE as a substrate (Fig. 1c). Besides, the previous reported MOMT2 could not catalyze KAE to produce detectable KDE in our assay (Fig. 1d), probably owing to its low activity to KAE. The uncharacterized GmOMT2 enzyme from the 19 newly cloned *G. max* MTs catalyzed C4'-OH methylation of 8P-KAE to icaritin, as determined by HPLC (Fig. 1c), HPLC/ESIMS, and NMR (Fig. S6a, b online). None of the other 18 GmOMTs converted 8P-KAE into icaritin (Fig. S6c online). Also, GmOMT2 catalyzed the C4'-OH methylation of KAE to KDE (Fig. 1d). However, the conversion ratio to KAE was < 1%, markedly lower than its activity for 8P-KAE (81.1%) (Fig. 1e). Therefore, GmOMT2 is suitable for constructing a microbial-fermentation-suitable icaritin biosynthetic pathway. The optimum pH and temperature for GmOMT2 were 9.5–10.0 and 35–40 °C, respectively (Fig. S7 online). The V_{max}, K_m, k_{cat}, and k_{cat}/K_m values of GmOMT2 with 8P-KAE as a substrate were 143.5 nmol min^{-1} mg^{-1}, 24.1 μmol L^{-1}, 0.16 s^{-1}, and 0.0066 L μmol^{-1} s^{-1}, respectively (Table S4 online). The activity of GmOMT2 decreased markedly at pH < 7.5, falling zero at pH < 6.5.

3.3. Construction of yeast strains that produce KAE from glucose

KAE is an intermediate for the biosynthesis of many bioactive flavonoids, including icaritin (Fig. 2). Therefore, we initially sought to develop a yeast strain with the capacity for high-level production of KAE. We chose yeast because no prenylation activity was detected upon expressing EsPT2 in *E. coli* (Fig. S8 online). The native yeast pathway from phenylpyruvate to phenylethanol catalyzed by PDC5 and ARO10 suppresses the accumulation of downstream phenylpropanoid compounds [37]. Therefore, we first

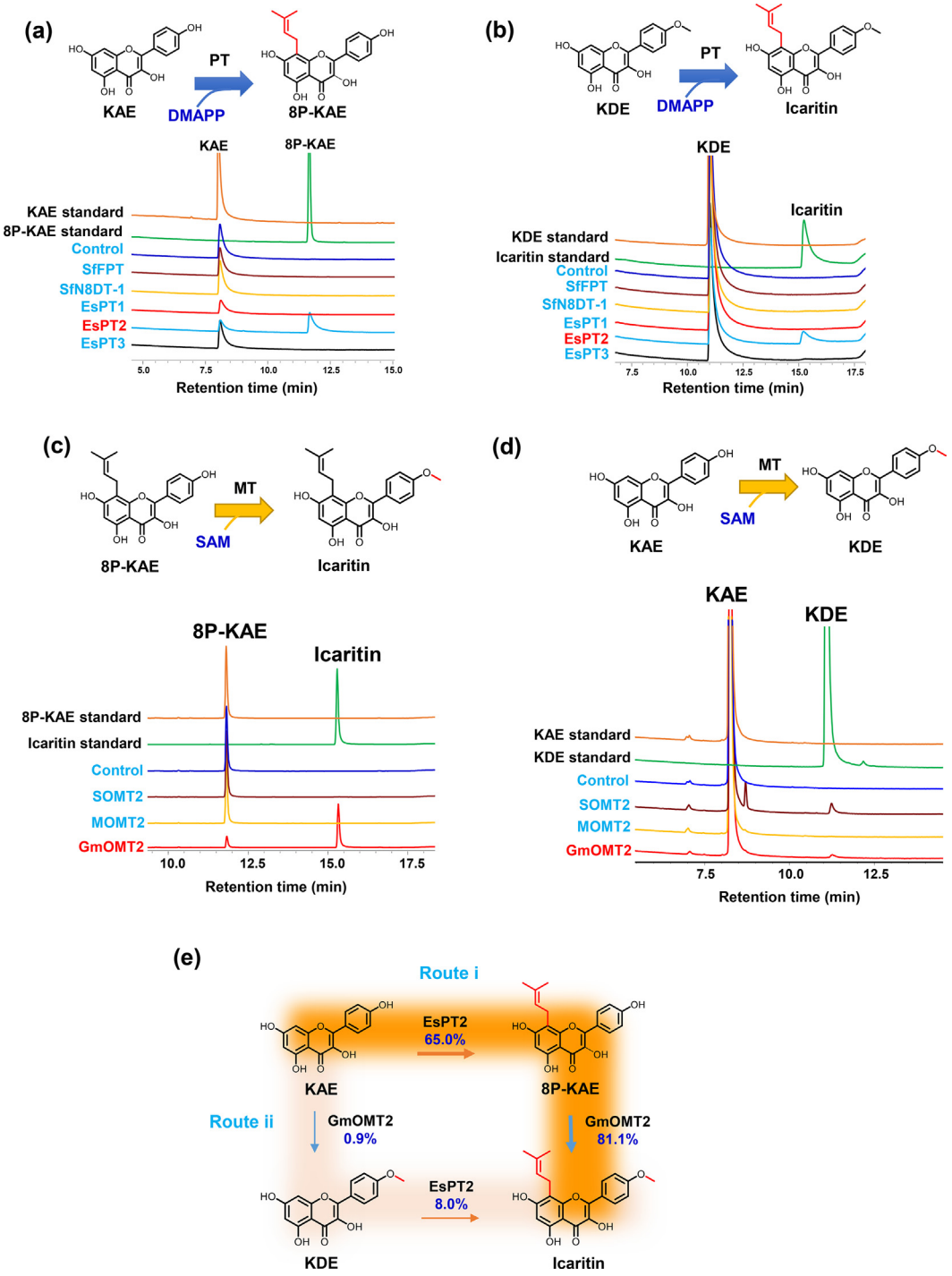

Fig. 1. Characterization of prenyltransferases and methyltransferases for the biosynthesis of icaritin. (a, b) Functional characterization of prenyltransferases involved in the C8 prenylation of flavonoids. Microsomal fractions of the yeast strains expressing each PTs (three PT candidates EsPT1-3 from *Epimedium sagittatum* and two previously reported naringenin PTs, SfN8DT-1 and SfFPT, both from *Sophora flavescens*) were incubated with KAE (a) and KDE (b) as a substrate and dimethylallyl pyrophosphate (DMAPP) as the prenyl donor, respectively. The *in vitro* assay products were monitored by HPLC analysis, authentic standards KAE, KDE, 8P-KAE, and icaritin were used for the detection and quantification of the prenylated flavonoid products; yeast with an empty pESC-HIS vector was used as a negative control. (c, d) Functional characterization of methyltransferases involved in the C4'-OH methylation of flavonoids. Crude extract of the *E. coli* strains expressing each MT (the MT candidate GmOMT2 from *G. max* and the two previous reported MTs, SOMT2 from *G. max* and MOMT2 from *Solanum habrochaites*) were incubated with 8P-KAE (c) and KAE (d) as a substrate and *S*-adenosylmethionine (SAM) as the methyl donor, respectively. The *in vitro* assay products were monitored by HPLC analysis, authentic standards KAE, KDE, 8P-KAE and icaritin were used for the detection and quantification of the methylated flavonoid products, *E. coli* with an empty pET28a vector was used as a negative control. (e) Proposed biosynthetic route of icaritin from KAE by EsPT2 and GmOMT2 based on their respective substrate conversion ratios. Route i (dark orange): KAE was first subjected to C8 prenylation by EsPT2, followed by the C4'-OH methylation by GmOMT2. Route ii (light orange): KAE was first subjected to C4'-OH methylation by GmOMT2, followed by C8 prenylation by EsPT2; the conversion ratio of each enzyme toward different substrates is labeled below the enzyme. KAE, kaempferol; 8P-KAE, 8-prenylkaempferol; KDE, kaempferide.

deleted these two genes, resulting in the starter strain WP125 (Figs. 2 and 3a). Next, we transformed WP125 with *FjTAL* from *F. johnsoniae* as well as with *4CL*, *CHS*, and *CHI* from *A. thaliana*; the resulting strain WP126 produced 3.7 mg/L NAR in shake flasks as determined by HPLC. Next, we expressed $ARO4^{K229L}$, $ARO7^{G141S}$ and an *E. coli* shikimate kinase II (*aroL*) to increase shikimate pathway activity. The resulting strain WP127 produced 7.2 mg/L NAR, a 95% increase over WP126. A sufficient supply of malonyl-CoA influences flavonoid-biosynthesis efficiency, so we overexpressed *ACC1* to increase the malonyl-CoA content and introduced an additional copy of *CHS* to enhance this step. The NAR yield of the resulting WP128 strain reached 18.4 mg/L, a value 250% higher than that of WP127 (Fig. 3a).

Although NAR production was increased significantly by the above engineering strategies, the final titer was very low. To identify the limiting step in NAR biosynthesis, we next fed strain WP128 with *p*-coumaric acid (pCA), L-tyrosine (L-Tyr), or L-phenylalanine (L-Phe) (all at 1 mmol/L). NAR production by WP128 reached 67.5, 23.1, and 17.4 mg/L, upon feeding with pCA, L-Tyr, and L-Phe, respectively. The feeding of L-Phe led to a slight decrease in NAR production, suggesting that L-Phe acts as a feedback suppressor of NAR synthesis in WP128. Feeding of L-Tyr led to a modest 26% increase in NAR production. Feeding with pCA almost quadrupled NAR production, indicating that conversion of L-Tyr to pCA limits the efficiency of NAR synthesis in strain WP128 (Fig. 3b).

To address this, we attempted to increase the expression level of *FjTAL* by introducing an additional copy of *FjTAL* and introducing another pathway of pCA synthesis from L-Phe by overexpressing *PAL*, *C4H*, and *ATR1* (an NADPH-cytochrome P450 reductase to support the function of C4H) from *A. thaliana*. The resulting strain WP129 produced 139.0 mg/L NAR, a 7.6-fold increase over WP128 (Fig. 3a and Fig. S9a, b online). In addition, no additional NAR production titers were obtained upon feeding WP129 with

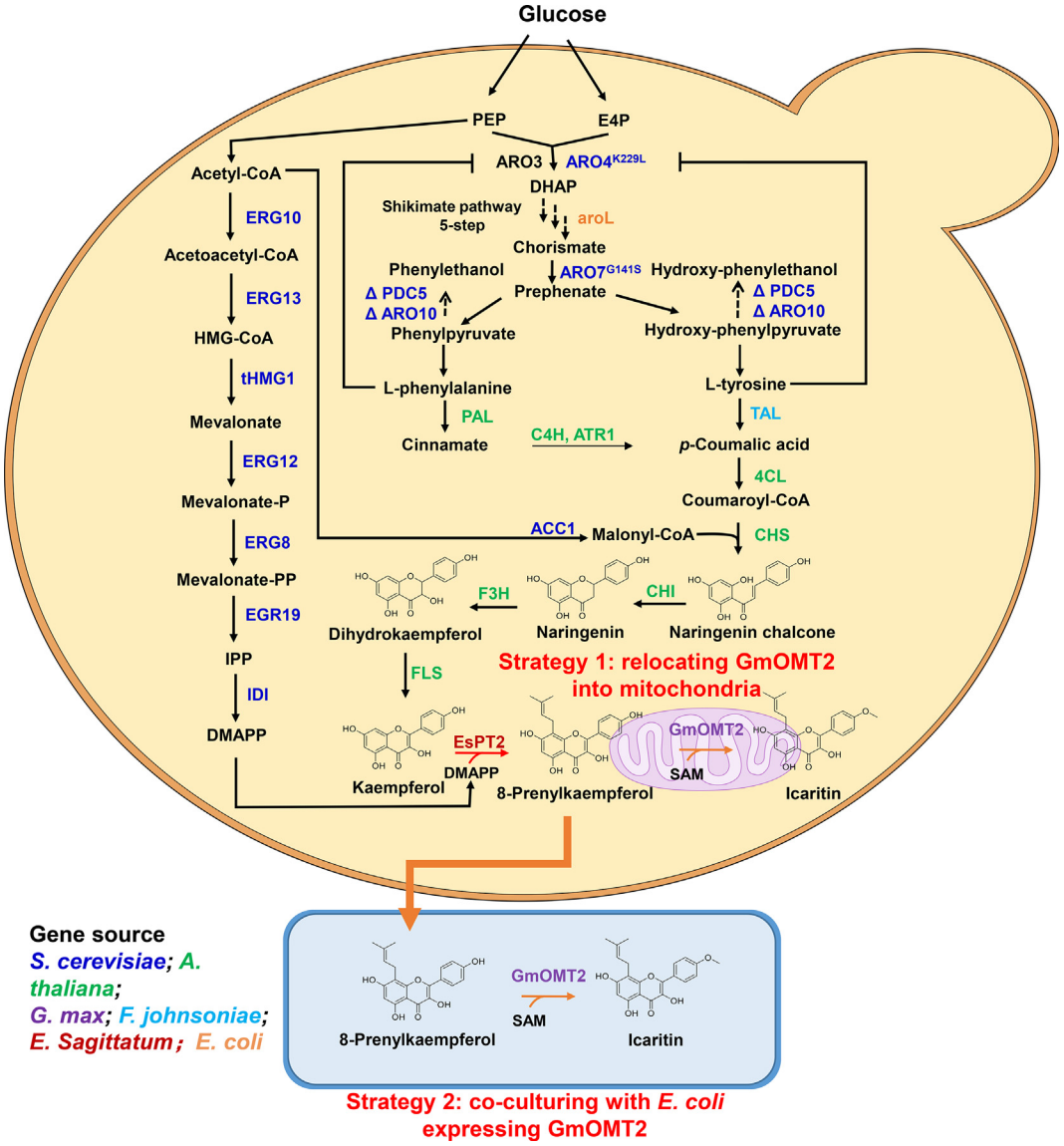

Fig. 2. Schematic illustrating the complete biosynthesis of icaritin from glucose by engineered *S. cerevisiae* and *E. coli* strains. Genes from different biological sources are shown in different colors. PAL, phenylalanine ammonia lyase; TAL, tyrosine ammonia lyase; C4H, cinnamate 4-hydroxylase; CPR, NADPH-cytochrome P450 reductase; 4CL, 4-coumaroyl-CoA ligase; CHS, chalcone synthase; CHI, chalcone isomerase; F3H, flavonol 3b-hydroxylase; FLS, flavonol synthase; DMAPP, dimethylallyl pyrophosphate; SAM, *S*-adenosylmethionine.

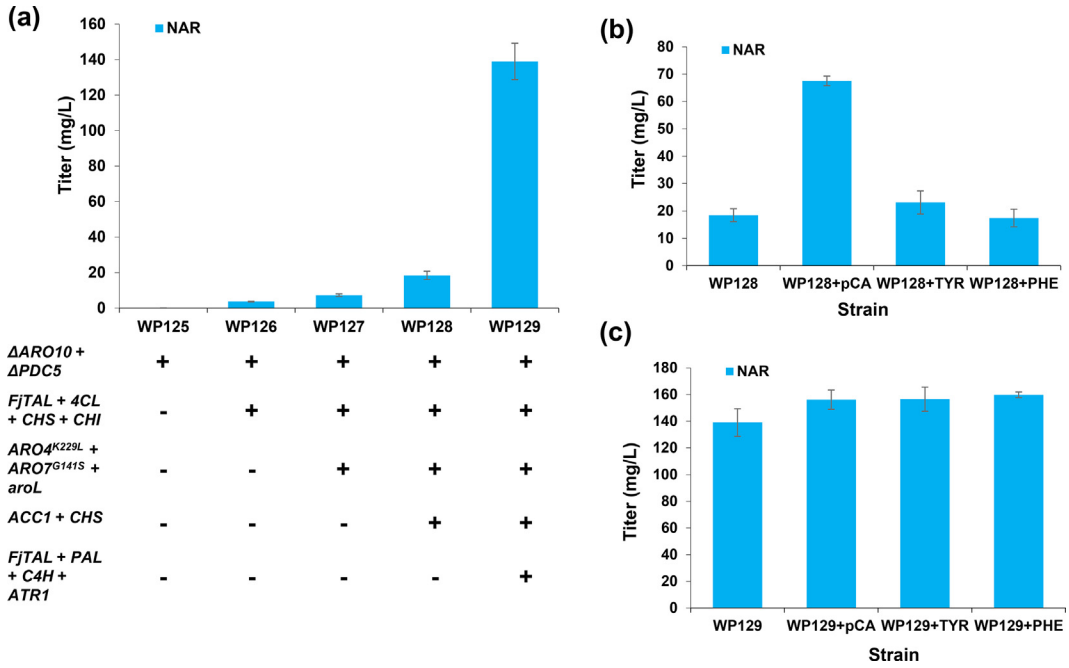

Fig. 3. (Color online) Engineering *S. cerevisiae* to generate a high-level naringenin production strain. (a) Naringenin (NAR) production by different engineered yeast strains in 10 mL shake flasks. (b) NAR production by the WP128 strain with or without 1 mmol/L of *p-coumaric* acid (pCA), L-tyrosine (L-Tyr), or L-phenylalanine (L-Phe) in 10 mL shake flasks. (c) NAR production by strain WP129 with or without 1 mmol/L of pCA, L-Tyr, or L-Phe in 10 mL shake flasks. Data are presented as mean ± standard deviation (SD) from three biological replicates. Student's two-tailed *t*-test, *P*-values between WP129 and WP129 + pCA, WP129 + TYR, WP129 + PHE were 0.08, 0.10, and 0.03, respectively.

L-Tyr, L-Phe, or pCA. Therefore, the engineering steps were successful and the conversion of L-Tyr into pCA was no longer pathway-limiting in the WP129 strain (Fig. 3c).

To generate a strain with increased KAE production, we next introduced the flavanone 3-hydroxylase gene *F3H* and the flavonol synthase gene *FLS* from *A. thaliana* into WP129 (Fig. 4a). The resulting strain WP130 produced 26.0 mg/L KAE, 49.7 mg/L dihydrokaempferol (DiKAE) and 57.3 mg/L NAR in shake flasks (Fig. 4b and Fig. S9a online). Considering the low efficiency of KAE biosynthesis from NAR, we replaced the *F3H* and *FLS* genes with the yeast codon-optimized genes *synF3H* and *synFLS*, which increased the KAE yield of the resulting strain WP131 to 119.7 mg/L, a 4.6-fold increase over WP130. Notably, the accumulation of the intermediate compound DiKAE decreased drastically to 4.6 mg/L in WP131 (vs. 49.7 mg/L for WP130). Further, introducing one additional copy each of *synF3H* and *synFLS* resulted in a slight increase in the KAE yield of the resulting WP132 strain to 151.5 mg/L (Fig. 4b and Fig. S9c online). To our knowledge, this strain with its *de novo* flavonoid pathway has the highest KAE yield of any engineered microbe. The results suggest that beyond their utility in icaritin biosynthesis, strains WP129 and WP132 could mediate the biosynthesis of other flavonoids, such as breviscapine and apigenin.

3.4. Construction of yeast strains that produce 8P-KAE from glucose

Having identified EsPT2 and with a KAE-producing yeast strain in hand, we next engineered an 8P-KAE–producing yeast strain. We introduced *EsPT2* under the control of a strong artificial promoter (*UAS-TDH* [38]) into WP132 to generate strain WP133. The 8P-KAE yield from WP133 was 1.2 mg/L (Fig. 5a, b and Fig. S10a online). Recall that plant prenyltransferases are membrane proteins that typically have at least seven transmembrane domains; these proteins also typically have an N-terminal plastid signal peptide. Truncation of N-terminal amino acids can increase the *in vivo* efficiency of PTs [39], so we generated three variants from which 10, 30, or 60 N-terminal amino acids were truncated (PT*tru10*, PT*tru30*, and PT*tru60*, respectively). These three truncation variants were introduced into WP132 under the control of the same promoter and terminator as the full-length *EsPT2*. The 8P-KAE production titers were respectively 3.51, 3.95, and 0.24 mg/L for the strains expressing the PT*tru10*, PT*tru30*, and PT*tru60* variants. Therefore, the variants lacking 10 and 30 N-terminal amino acids conferred significantly higher 8P-KAE yields than full-length *EsPT2*. The best-performing strain was WP132 harboring PT*tru30* (hereafter, WP134), which exhibited a 3.3-fold increase in 8P-KAE yield compared to the WP133 strain (Fig. 5a, b and Fig. S10a online).

The above results confirmed that EsPT2 needs the mevalonate pathway intermediate DMAPP as a phenyl donor, so we overexpressed the seven enzymes in the mevalonate pathway from acetyl-CoA to DMAPP (ERG10, ERG13, tHMG1, ERG12, ERG8, ERG19, and IDI) in strain WP134, generating the WP135 strain (Fig. 5a). The 8P-KAE yield increased to 25.9 mg/L, a 6.6-fold increase over WP134 (Fig. 5b). A time-course analysis of the growth and flavonoid production of WP135 revealed that the KAE level stopped increasing after 36 h and decreased from 70.2 to 12.1 mg/L at 48 h (Fig. S10b online); however, the 8P-KAE yield increased by only 4.9 mg/L from 36 to 48 h, indicating that the majority of KAE was not converted to 8P-KAE. Coincidentally, the decrease in the KAE level from 36 to 48 h was correlated with the transition from log to stationary phase. The mechanism underlying this phenomenon is unclear to us, as is its correlation with the growth-phase transition. The marked decrease in the KAE level may be caused by degradation by native enzymes, as reported in *E. coli* and in other fungi [40,41], or by the formation of undetectable protein–flavonoid complexes [42] when the total flavonoids reach a threshold level. Beyond demonstrating the first production of 8P-KAE in yeast, this result is important because it represents the highest reported yield of a prenylated flavonoid via an artificial pathway in engineered microbes.

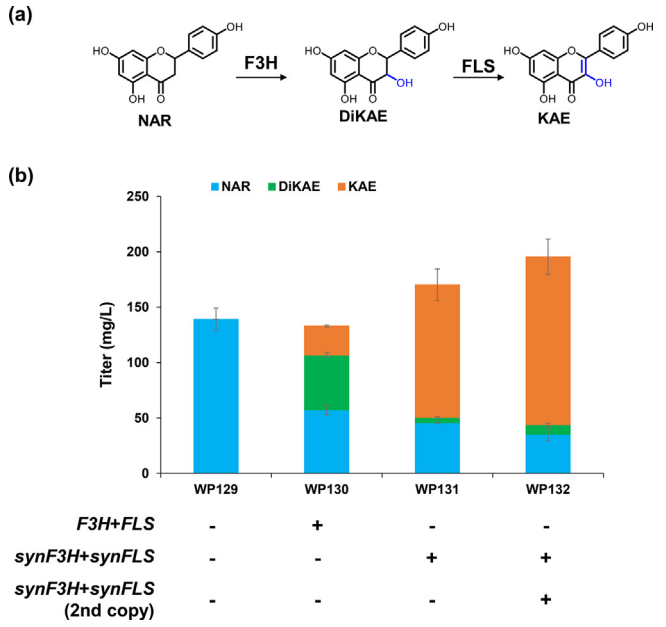

Fig. 4. Engineering *S. cerevisiae* to generate a high-level kaempferol production strain. (a) Biosynthetic pathway of KAE from NAR, flavonol 3b-hydroxylase (F3H) and flavonol synthase (FLS) both of which are from *A. thaliana*. (b) NAR, DiKAE, and KAE production by engineered yeast strains in 10 mL shake flasks. Values are presented as mean ± SD from three biological replicates. NAR, naringenin; DiKAE, dihydrokaempferol; KAE, kaempferol.

3.5. Complete biosynthesis of icaritin from glucose in a yeast by relocating GmOMT2 into mitochondria

We next attempted to produce icaritin by introducing GmOMT2 into the WP135 strain; however, neither icaritin nor other new compounds were produced, despite enhancement of GmOMT2 expression by codon optimization, GST tag fusion, N-terminus truncation, and feeding with 0.5 mmol/L SAM (Fig. S11 online). Given that the cytoplasmic pH of yeast is typically ~5.5–7 [43] and the C4′,-OH methylation activity of GmOMT2 was markedly decreased at pH 7.5 and undetectable at pH < 6.5 (Fig. S7 online), the low pH in yeast cells may suppress GmOMT2 activity. However, adjusting the pH value of the fermentation medium did not solve the problem, because yeast intracellular pH is unaffected by external pH [43].

The mitochondrial pH is higher than that in the cytoplasm in *S. cerevisiae* [44], so we envisioned that relocating GmOMT2 into yeast mitochondria may enable GmOMT2 to function in yeast. Six mitochondrial localization signal peptides (ATPA, COX4, GLRX2, MAM33, ODPA, and ODPB) were fused with the N-terminus of a yeast-codon-optimized variant of *GmOMT2* and introduced into a wild-type yeast strain. The resulting six strains, a yeast strain harboring GmOMT2 without an MLS tag, and the wild-type yeast, were cultivated and fed 20 mg/L 8P-KAE. Strains harboring GmOMT2 fused to the ATPA, GLRX2, and MAM33 tags produced icaritin; the strain with ATPA-tagged GmOMT2 had the highest conversion ratio (36.4%) (Fig. S12 online). No icaritin was produced by strains harboring untagged GmOMT2 or the other tagged GmOMT2 variants. Therefore, localization of GmOMT2 into the relatively higher pH context of mitochondria overcomes any low pH-mediated restriction. We subsequently achieved icaritin biosynthesis in yeast by introducing the ATPA-tagged GmOMT2 variant into WP135. HPLC revealed that the resulting WP137 strain had an icaritin yield of 7.2 mg/L (Fig. 5c). Fluorescence microscopy using Mitotracker red verified the mitochondrial localization of an N-terminal ATPA- and GFP-tagged GmOMT2 variant (APTA-GFP-yeGmOMT2) (Fig. 5d).

3.6. Complete biosynthesis of icaritin from glucose by co-culturing of the engineered yeast and E. coli strains

Given our aforementioned results for successful expression of GmOMT2 in *E. coli*, we also attempted to circumvent the apparently weak of GmOMT2 activity in yeast by distributing the icaritin pathway into two hosts, with the terminal 4'-OH methylation step occurring in *E. coli*. To this end, we co-cultured engineered yeast and *E. coli* strains so that the biotransformation of glucose to 8P-KAE took place in yeast, followed by the conversion of 8P-KAE to icaritin in *E. coli* (Fig. 5e).

To improve methylation efficiency, we first optimized the expression of GmOMT2 in *E. coli* by fusing GmOMT2 with an N-terminal GST tag, a technique commonly used to improve the soluble expression of heterologous proteins in *E. coli*, generating the WPE4 strain. Whole-cell catalysis assays indicted that the conversion ratio of 8P-KAE (50 mg/L feed) into icaritin by WPE4 was 46.4%, a 45% increase compared to WPE3 (31.9%) with wild-type GmOMT2 (Fig. S13 online). *E. coli* codon optimization of the GmOMT2 fusion resulted in generation the WPE5 strain; its conversion rate was 71.3%, more than twofold higher than that of WPE3 (Fig. S13 online).

We next co-cultured the 8P-KAE–producing strain WP135 and the methylation strain WPE5. Specifically, WP135 was initially incubated in YPD medium and fermented at 30 °C for 72 h. Subsequently, WPE5 that had been induced by IPTG in LB medium was collected, suspended in fresh LB medium, and added to the WP135 fermentation broth at the end of the initial 72 h culture. The mixed strains were co-cultured at 30 °C for 24 h, and the flavonoid products were extracted and monitored by HPLC (Fig. 5f). A peak with a retention time identical to the icaritin reference standard was detected in the WP135/WPE5 co-culture; no such peak was detected in the negative control (co-culture of WP135 with *E. coli* BL21 harboring an empty pET28a plasmid). Therefore, icaritin was synthesized by combining strains WP135 and WPE5, and the yield was 19.7 mg/L.

Time course analysis of the co-culturing system revealed that icaritin kept increasing within 24 h, reaching its highest production level at 96 h of co-culture (Fig. S14a online). The levels of 8P-KAE and icaritin decreased with increasing WP135/WPE5 culture duration. In the control for WP135/BL21emp co-culture the 8P-KAE level decreased markedly after 96 h, and it was absent after 120 h (Fig. S14b online). The mechanism of this phenomenon may be similar to that of the decrease in KAE in WP135 monoculture.

The tolerance of microbial strains for flavonoids is unclear. When the total flavonoids in microbial cell factories reach a threshold, the degradation or conversion of flavonoids may be activated. *Penicillium* and *Aspergillus* fungi undertake quercetinase-mediated breakdown of flavonoid skeletons, leading to synthesis of phenolic acids [40]. Also, the *E. coli* protein YhhW (quercetin 2,3-dioxygenase) has quercetinase activity, suggesting that *E. coli* is capable of degrading flavonoids[41]. Some flavonoids, including KAE, form undetectable protein–flavonoid complexes by interacting with the free amino-, sulfhydryl groups and tryptophan side chains of proteins [42]. Further studies of the mechanism of the decreased flavonoid levels in yeast and *E. coli* are needed to overcome the issue of flavonoid disappearance and so increase icaritin production. Icaritin production could also likely be improved by optimizing the fermentation conditions for WP137 monoculture or WP135 and WPE5 co-culture in bioreactors.

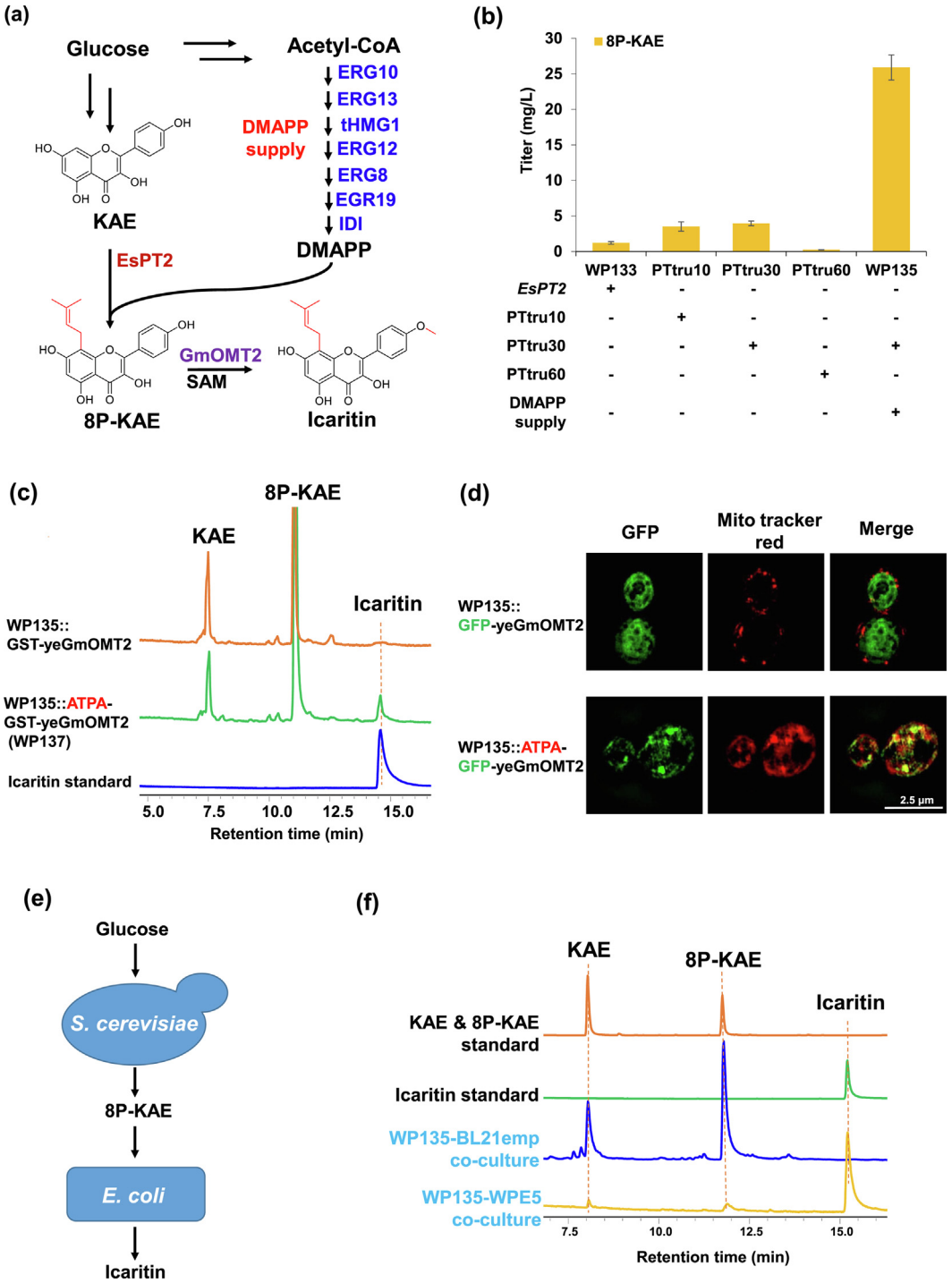

Fig. 5. Complete biosynthesis of icaritin from glucose by engineered microbial strains. (a) Schematic illustrating the engineering strategies for improving 8P-KAE production and its conversion into icaritin in a single *S. cerevisiae* strain. (b) Quantification of 8P-KAE production by different engineered yeast strain in 10 mL shake flasks. (c) HPLC analysis of flavonoid production by different engineered yeast strains in 10 mL shake flasks. WP135::GST-yeGmOMT2, WP135 strain expressing N terminal GST tagged yeast codon-optimized *GmOMT2* gene. WP135::APTA-GST-yeGmOMT2 (WP137), WP135 strain expressing N terminal APTA and GST tagged yeast codon-optimized *GmOMT2* gene. (d) Fluorescence microscopy of yeast strains. WP135::GFP-yeGmOMT2, WP135 strain expressing N terminal GFP tagged yeast codon-optimized *GmOMT2* gene. WP135:: APTA-GFP-yeGmOMT2, WP135 strain expressing N terminal APTA and GFP tagged yeast codon-optimized *GmOMT2* gene. (e) Schematic illustrating of complete biosynthesis of icaritin from glucose. Briefly, the upstream pathway from glucose to 8P-KAE was fulfilled in engineered yeast, and then 8P-KAE was converted into icaritin by *E. coli* expressing GmOMT2. (f) HPLC analysis of flavonoid products produced from co-cultures comprising the engineered yeast strain WP135 with *E. coli* strain WPE5. Co-culturing of yeast strain WP135 with *E. coli* strain BL21 harboring empty pET-28a vector (BL21emp) was performed as a negative control. Authentic standard KAE, 8P-KAE, and icaritin were used for the detection and quantification of the corresponding flavonoid products. Values are presented as mean ± SD from three biological replicates. KAE, kaempferol; 8P-KAE, 8-prenylkaempferol.

4. Conclusion

We identified a previously unreported prenyltransferase (EsPT2) from the *Berberidaceae*-family plant *E. sagittatum* and a previously uncharacterized methyltransferase (GmOMT2) from *G. max*, which catalyzed the C8 prenylation of KAE to yield 8P-KAE and the C4',OH methylation of 8P-KAE to synthesize icaritin, respectively. Using EsPT2 and GmOMT2, we created an artificial biosynthetic pathway for icaritin comprising genes from *S. cerevisiae*, *A. thaliana*, *E. coli*, *G. max*, *F. johnsoniae*, and *E. sagittatum* by two strategies. In strategy 1, we generated a yeast strain that produces icaritin from glucose by relocating GmOMT2 into the mitochondria of 8P-KAE-producing yeast cells. In strategy 2, we used a co-culture system that achieved an icaritin level of 19.7 mg/L with glucose as the substrate by dividing the synthetic pathway into *S. cerevisiae* and *E. coli*. Our work will enable realization of industrial-scale production of icaritin, and further engineering to produce icaritin derivatives (e.g., icariside I, icariside II, icariin, epmedin A, epmedin B, and epmedin C) by introducing glucosyltransferase enzymes and pathways to produce sugar donors. We also illustrated how strain engineering by exploring organelle localization and process engineering by utilizing two host species to overcome the widespread issue of pH mediated incompatibility of heterogonous enzymes and eukaryotic chasses encountered in basic and applied biology research.

Conflict of interest

The authors declare that they have no conflict of interest.

Acknowledgments

This work was supported by the National Key Research and Development Program of China (2018YFA0900700), the National Natural Science Foundation of China (31901021 and 31921006), the Strategic Priority Research Program of the Chinese Academy of Sciences (XDB27020206), the International Partnership Program of Chinese Academy of Sciences (153D31KYSB20170121), and the Strategic Biological Resources Service Network Plan of the Chinese Academy of Sciences (KFJ-BRP-009). The authors thank Dr. Yining Liu (Core Facility Center of the Institute of Plant Physiology and Ecology) for mass spectrometry assistance.

Author contributions

Zhihua Zhou, Ying Wang, and Xing Yan designed and supervised this study. Pingping Wang and Chaojing Li performed flavonoids *S. cerevisiae* and *E. coli* strain engineering. Pingping Wang, Wenjun Huang, and Jiali Wang carried out the cloning and characterization of prenyltransferases. Xiaodong Li and Xing Yan performed the cloning and characterization of methyltransferases. Yan Wang performed the NMR analysis of the products. Xiaoman Yang and Yanjun Zhang provided transcriptome dataset. Pingping Wang and Zhihua Zhou wrote the manuscript.

Appendix A. Supplementary materials

Supplementary materials to this article can be found online at https://doi.org/10.1016/j.scib.2021.03.002.

References

[1] Ma HP, He XR, Yang Y, et al. The genus *Epimedium*: an ethnopharmacological and phytochemical review. J Ethnopharmacol 2011;134:519–41.
[2] Indran IR, Liang RLZ, Min TE, et al. Preclinical studies and clinical evaluation of compounds from the genus *Epimedium* for osteoporosis and bone health. Pharmacol Therapeut 2016;162:188–205.
[3] Zhai YK, Guo X, Pan YL, et al. A systematic review of the efficacy and pharmacological profile of *Herba Epimedii* in osteoporosis therapy. Pharmazie 2013;68:713–22.
[4] Wang LL, Li Y, Guo YB, et al. *Herba Epimedii*: an ancient Chinese herbal medicine in the prevention and treatment of osteoporosis. Curr Pharm Des 2016;22:328–49.
[5] Huang H, Liang M, Zhang X, et al. Simultaneous determination of nine flavonoids and qualitative evaluation of *Herba Epimedii* by high performance liquid chromatography with ultraviolet detection. J Sep Sci 2007;30:3207–13.
[6] Li CR, Li Q, Mei QB, et al. Pharmacological effects and pharmacokinetic properties of icariin, the major bioactive component in *Herba Epimedii*. Life Sci 2015;126:57–68.
[7] Huang L, Wang XL, Cao HJ, et al. A bone-targeting delivery system carrying osteogenic phytomolecule icaritin prevents osteoporosis in mice. Biomaterials 2018;182:58–71.
[8] Zhu JF, Li ZJ, Sen Zhang G, et al. Icaritin shows potent anti-leukemia activity on chronic myeloid leukemia *in vitro* and *in vivo* by regulating MAPK/ERK/JNK and JAK2/STAT3/SKT signalings. PLoS One 2011;6:e23720.
[9] Zhao H, Guo YM, Li S, et al. A novel anti-cancer agent Icaritin suppresses hepatocellular carcinoma initiation and malignant growth through the IL-6/Gak2/Stat3 pathway. Oncotarget 2015;6:31927–43.
[10] Fan Y, Li S, Ding XY, et al. First-in-class immune-modulating small molecule Icaritin in advanced hepatocellular carcinoma: preliminary results of safety, durable survival and immune biomarkers. BMC Cancer 2019;19:279–89.
[11] Qin SK, Li Q, Xu JM, et al. Icaritin-induced immunomodulatory efficacy in advanced hepatitis B virus-related hepatocellular carcinoma: immunodynamic biomarkers and overall survival. Cancer Sci 2020;111:4218–31.
[12] Xu Y, Li Z, Wang Y. Fourteen microsatellite loci for the Chinese medicinal plant *Epimedium sagittatum* and cross-species application in other medicinal species. Mol Ecol Resour 2008;8:640–2.
[13] Nguyen VS, Shi L, Li Y, et al. Total synthesis of Icaritin via microwave-assistance claisen rearrangement. Lett Org Chem 2014;11:677–81.
[14] Paddon CJ, Westfall PJ, Pitera DJ, et al. High-level semi-synthetic production of the potent antimalarial artemisinin. Nature 2013;496:528–32.
[15] Yan X, Fan Y, Wei W, et al. Production of bioactive ginsenoside compound K in metabolically engineered yeast. Cell Res 2014;24:770–3.
[16] Wang PP, Wei YJ, Fan Y, et al. Production of bioactive ginsenosides Rh2 and Rg3 by metabolically engineered yeasts. Metab Eng 2015;29:97–105.
[17] Pandey RP, Parajuli P, Koffas MAG, et al. Microbial production of natural and non-natural flavonoids: pathway engineering, directed evolution and systems/synthetic biology. Biotechnol Adv 2016;34:634–62.
[18] Wu JJ, Zhou TT, Du GC, et al. Modular optimization of heterologous pathways for *de novo* synthesis of (2S)-naringenin in *Escherichia coli*. PLoS One 2014;9:e101492.
[19] Trantas E, Panopoulos N, Ververidis F. Metabolic engineering of the complete pathway leading to heterologous biosynthesis of various flavonoids and stilbenoids in *Saccharomyces cerevisiae*. Metab Eng 2009;11:355–66.
[20] Lyu XM, Zhao GL, Ng KR, et al. Metabolic engineering of *Saccharomyces cerevisiae* for *de novo* production of kaempferol. J Agr Food Chem 2019;67:5596–606.
[21] Levisson M, Araya-Cloutier C, de Bruijn WJC, et al. Toward developing a yeast cell factory for the production of prenylated flavonoids. J Agr Food Chem 2019;67:13478–86.
[22] Jones JA, Wang X. Use of bacterial co-cultures for the efficient production of chemicals. Curr Opin Biotech 2018;53:33–8.
[23] Zhou K, Qiao KJ, Edgar S, et al. Distributing a metabolic pathway among a microbial consortium enhances production of natural products. Nat Biotechnol 2015;33:377–U157.
[24] Wang EX, Ding MZ, Ma Q, et al. Reorganization of a synthetic microbial consortium for one-step vitamin C fermentation. Microb Cell Fact 2016;15:21.
[25] Huang WJ, Zeng SH, Xiao G, et al. Elucidating the biosynthetic and regulatory mechanisms of flavonoid-derived bioactive components in *Epimedium sagittatum*. Front Plant Sci 2015;6:689–701.
[26] Feng KP, Chen RD, Xie KB, et al. A regiospecific rhamnosyltransferase from *Epimedium pseudowushanense* catalyzes the 3-*O*-rhamnosylation of prenylflavonols. Org Biomol Chem 2018;16:452–8.
[27] Feng KP, Chen RD, Xie KB, et al. Ep7GT, a glycosyltransferase with sugar donor flexibility from *Epimedium pseudowushanense*, catalyzes the 7-*O*-glycosylation of baohuoside. Org Biomol Chem 2019;17:8106–14.
[28] Chen RD, Liu X, Zou JH, et al. Regio- and stereospecific prenylation of flavonoids by sophora flavescens prenyltransferase. Adv Synth Catal 2013;355:1817–28.

[29] Kim JH, Cho IS, So YK, et al. Kushenol A and 8-prenylkaempferol, tyrosinase inhibitors, derived from *Sophora flavescens*. J Enzyme Inhib Med Chem 2018;33:1048–54.
[30] Dell'Agli M, Galli GV, Dal Cero E, et al. Potent inhibition of human phosphodiesterase-5 by Icariin derivatives. J Nat Prod 2008;71:1513–7.
[31] Sasaki K, Mito K, Ohara K, et al. Cloning and characterization of naringenin 8-prenyltransferase, a flavonoid-specific prenyltransferase of *Sophora flavescens*. Plant Physiol 2008;146:1075–84.
[32] Sasaki K, Tsurumaru Y, Yazaki K. Prenylation of flavonoids by bio-transformation of yeast expressing plant membrane-bound prenyltransferase SfN8DT-1. Biosci Biotech Biochem 2009;73:759–61.
[33] Sasaki K, Tsurumaru Y, Yamamoto H, et al. Molecular characterization of a membrane-bound prenyltransferase specific for isoflavone from *Sophora flavescens*. J Biol Chem 2011;286:24125–34.
[34] Krogh A, Larsson B, von Heijne G, et al. Predicting transmembrane protein topology with a hidden markov model: application to complete genomes. J Mol Biol 2001;305:567–80.
[35] Kim DH, Kim BG, Lee Y, et al. Regiospecific methylation of naringenin to ponciretin by soybean *O*-methyltransferase expressed in *Escherichia coli*. J Biotechnol 2005;119:155–62.
[36] Schmidt A, Li C, Shi F, et al. Polymethylated myricetin in trichomes of the wild tomato species *Solanum habrochaites* and characterization of trichome-specific 3′/5′-and 7/4′-myricetin *O*-methyltransferases. Plant Physiol 2011;155:1999–2009.
[37] Rodriguez A, Kildegaard KR, Li MJ, et al. Establishment of a yeast platform strain for production of *p*-coumaric acid through metabolic engineering of aromatic amino acid biosynthesis. Metab Eng 2015;31:181–8.
[38] Blazeck J, Garg R, Reed B, et al. Controlling promoter strength and regulation in *Saccharomyces cerevisiae* using synthetic hybrid promoters. Biotechnol Bioeng 2012;109:2884–95.
[39] Li HX, Ban ZN, Qin H, et al. A heteromeric membrane-bound prenyltransferase complex from hop catalyzes three sequential aromatic prenylations in the bitter acid pathway. Plant Physiol 2015;167:650–9.
[40] Tranchimand S, Brouant P, Iacazio G. The rutin catabolic pathway with special emphasis on quercetinase. Biodegradation 2010;21:833–59.
[41] Adams M, Jia ZC. Structural and biochemical analysis reveal pirins to possess quercetinase activity. J Biol Chem 2005;280:28675–82.
[42] Kroll J, Rawel HM, Rohn S. Reactions of plant phenolics with food proteins and enzymes under special consideration of covalent bonds. Food Sci Technol 2003;9:205–18.
[43] Orij R, Urbanus ML, Vizeacoumar FJ, et al. Genome-wide analysis of intracellular ph reveals quantitative control of cell division rate by pH_C in *Saccharomyces cerevisiae*. Genome Biol 2012;13:R80.
[44] Orij R, Postmus J, Ter Beek A, et al. *In vivo* measurement of cytosolic and mitochondrial pH using a pH-sensitive GFP derivative in *Saccharomyces cerevisiae* reveals a relation between intracellular pH and growth. Microbiol 2009;155:268–78.

Pingping Wang is an assistant professor at the CAS Center for Excellence in Molecular Plant Sciences (CEMPS), Institute of Plant Physiology and Ecology, Chinese Academy of Sciences. He obtained his Ph.D. degree from University of Chinese Academy of Sciences in 2017. After that he conducted two years postdoctoral research and joined CEMPS in 2019. His research interest is yeast metabolic engineering and natural product synthetic biology.

Chaojing Li obtained her bachelor's degree from the School of Life Sciences, Henan University in 2016. She is a Ph.D. candidate in Prof. Zhihua Zhou's research group at CEMPS, Institute of Plant Physiology and Ecology, Chinese Academy of Sciences. Her research interest is plant natural products synthetic biology.

Xiaodong Li is a Ph.D. candidate in Microbiology at CEMPS, Institute of Plant Physiology and Ecology, Chinese Academy of Sciences. He received his bachelor's degree from Northwestern Polytechnical University in 2015. His research interest is plant natural products synthetic biology.

Wenjun Huang is an associate professor at the Wuhan Botanical Garden of the Chinese Academy of Sciences. He obtained his Ph.D. degree from Wuhan Botanical Garden of the Chinese Academy of Sciences in 2011. After that, he joined Prof. Ying Wang's research group. His research interest is flavonoid metabolism, germplasm resources, and breeding of kiwifruit.

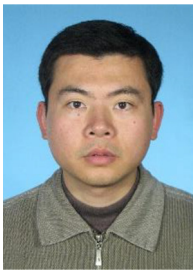

Xing Yan is a professor at CEMPS, Institute of Plant Physiology and Ecology, Chinese Academy of Sciences. He obtained his Ph.D. degree from Shanghai Jiao Tong University in 2007. After that, he joined Prof. Zhihua Zhou's research group at CEMPS. His research interest is natural product synthetic biology and bioparts database construction.

Ying Wang is a professor at Center of Economic Botany, Core Botanical Gardens, Chinese Academy of Sciences. She received her Ph.D. degree from Clemson University in 2002. After that, she conducted three years postdoctoral research in Cornell University. She is now a principal investigator and led the Secondary Metabolism and Genetic Breeding of Medicinal Plants research group. Her research interest is molecular genetics of medicinal plants.

Zhihua Zhou is a professor at CEMPS, Institute of Plant Physiology and Ecology, Chinese Academy of Sciences. She received her Ph.D. degree from the University of Tokyo in 2000. She became a principal investigator and led the Fungi Molecular Genetics and Synthetic Biology research group at CEMPS in 2015. Her research interest includes natural product synthetic biology and filamentous fungi molecular genetics.